Polymer Vol. 38 No. 12, pp. 2907–2923, 1997

0032-3861/97/$17.00 + 0.00

PII: S0032-3861(96)00848-8

Texture of injection moulded poly(ethylene-2,6-naphthalene dicarboxylate) parts

Y. Ülçer and M. Cakmak*
Polymer Engineering Institute, College of Polymer Science and Polymer Engineering, The University of Akron, Akron, OH 44325-0301, USA
(Received 9 January 1996; revised 2 August 1996)

Evolution of structural gradients developed in injection moulded polyethylene naphthalate was studied using a variety of structural techniques including a newly developed micro-beam X-ray diffraction pole figure technique. PEN, being a slowly crystallizing high temperature polymer, forms a three layer structure: amorphous skin + shear crystallized intermediate layer + amorphous core in the interior at low mould temperatures. The thickness of the crystallized sublayers formed under the action of flow decrease with the increase of mould temperature as a result of reduction of stress history experienced by the flowing polymer chains. Their thickness increases in the narrow passages of the cavity as a result of increased fraction of the extensional component of the flow field which locally causes increases in crystallization rates. The crystalline structure of these layers were found to contain both α and β phases. The hot stage-WAXS experiments indicate that the β phase possess a melting temperature approximately 30°C higher than the α form. In the shear crystallized regions, the polymer chains are oriented along the flow direction and the naphthalene planes that are flexibly linked together along the polymer chain tend to be oriented parallel to the broad surfaces of the part. The preferential alignment of the naphthalene planes results in highly layered macrostructure in the shear crystallized zones with weak interlayer forces. As a result, these regions readily delaminate into plate-like structures observed in the SEM fracture surfaces. © 1997 Elsevier Science Ltd.

(Keywords: poly(ethylene-2,6-naphthalate); injection moulding; polymorphism)

INTRODUCTION

Poly(ethylene-2,6-naphthalate) (PEN) is a relatively new engineering thermoplastic that was developed by ICI in 1948[1]. It has the chemical structure

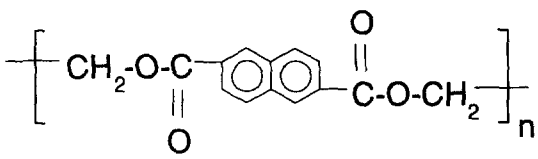

PEN is known to have two crystal forms, named α- and β-forms by Buchner *et al.*[2]. The crystal structure of the α-form of PEN was determined by Mencik[3]. Its triclinic unit cell contains one chain and has the unit cell parameters $a = 6.51$ Å, $b = 5.75$ Å, $c = 13.2$ Å with $\alpha = 81.33°$, $\beta = 144°$ and $\gamma = 100°$. The α-form of PEN belongs to the $P\bar{1}$ space group. The formation of a second crystal structure having a higher melting point and better mechanical properties during special spinning or annealing process was noted in the patent literature[4]. Zachmann[5] observed the development of this crystal structure during isothermal crystallization above 245°C by synchrotron radiation. Later Buchner *et al.*[2] reported that a unit cell of this new form (β-form) is also triclinic and has dimensions $a = 9.26$ Å, $b = 15.59$ Å, $c = 12.73$ Å, $\alpha = 121.6°$, $\beta = 95.57°$ and $\gamma = 122.52°$. In the β-form, four chains pass through each unit cell. They indicate that the chains are not fully extended and every other naphthalene plane rotates 180° about the chain axis. However, detailed crystallographic information on this phase is currently still lacking.

The development of orientation in uniaxially and biaxially stretched PEN films has been studied in detail[6–9]. It has been observed that in both uniaxially and biaxially stretched films, PEN crystallizes in the α-form and the naphthalene rings tend to orient parallel to the film surface. In a recent study, Cakmak and Kim[9] observed β-form crystals in PEN fibres spun at high speeds.

In our previous paper, we studied the effect of processing conditions on the morphology of the injection moulded PEN parts[10]. We have found that, PEN exhibits a three layer structural gradient consisting of an amorphous skin, a shear crystallized intermediate layer and an amorphous core, at mould temperatures up to its glass transition temperature. When examined with differential scanning calorimetry (d.s.c.) technique, the shear crystallized layers were found to exhibit a small population of crystals with high melting temperature (~300°C) in addition to the regular crystals that melt around 270°C.

In this paper, hot stage WAXS, micro-beam WAXS and a new micro-beam WAXS pole figure technique were used in order to identify and quantify the details of the texture of the shear crystallized layers in injection moulded parts.

* To whom correspondence should be addressed

EXPERIMENTAL

Material

PEN used in this study was provided by Goodyear Co. under the trade name Traytuf HP, VFR40008X. It is an injection moulding grade having an intrinsic viscosity of 0.824 dl g^{-1}. PEN pellets were dried in a vacuum oven at 145°C for at least 24 h and processed immediately after drying.

Injection moulding

End gated ASTM small dumbbells were injection moulded at four different mould temperatures, namely 20, 90, 120 and 180°C, using a Boy 15S injection moulding machine. All other processing variables are summarized in *Table 1*. Details of the injection moulding process and schematics of the mould cavity can be found in our first paper[10].

Cutting procedures

To characterize the structure of the injection moulded test bars three sectioning procedures were used (*Figure 1*). Procedure A involved cutting sections of *ca.* 0.6 mm thickness perpendicular to the flow direction in the transverse direction–normal direction (TD–ND) plane. Procedure B consisted of cutting a slice along the centre-line of the specimen in the flow direction–normal direction (FD–ND) plane. In Procedure C, a thick section cut using Procedure A, was sectioned parallel to the flow direction in the FD–TD plane. The samples were cut using a Leco VC-50 diamond saw.

Optical microscopy

Transmission optical photomicrographs of the regions, where the micro beam WAXS patterns are obtained, were taken using a digital camera (Sony 3CCD) and video printer (Sony UP300) setup attached to a Leitz Laborlux POL12S microscope. These photographs were used to match the X-ray data with the optical observations.

Wide angle X-ray diffraction (WAXS)

Film patterns. For crystal structure determination, WAXS film patterns of the injection moulded samples were taken from location No. 3 of the B cut samples using a Furnas WAXS/SAXS Camera. The camera was attached to a GE XRD-6 copper target X-ray generator that was operated at 40 kV and 30 mA. The CuK_α beam having a 0.75 mm diameter was monochromatized using a nickel foil filter. The sample to film distance was 5.27 cm. Exposure times were varied from 3 to 12 h in order to identify the locations of largest possible numbers of planes.

To investigate the micro-structural variation from skin to core, B-cut samples were mounted on the precision X–Y stage of the X-ray camera (MMBX) developed in our laboratories. The orientation of the sample was such that the incident X-ray beam became parallel to the transverse direction (*Figure 2*). The camera was mounted on a Rigaku RU-200B rotating anode X-ray generator, that was operated at 40 kV and 150 mA. The CuK_α radiation was collimated to 100 μm and monochromatized using a nickel foil filter. The sample to film distance was around 1.52 cm and typical exposure times were kept around 1 h 15 min.

WAXS pole figures. It has been experimentally observed that both amorphous and semi-crystalline polymers show structural gradients from skin to core due to the combined effect of flow and cooling[11–13]. These variations are shown to be more pronounced especially in the shear layers adjacent to the skin where the temperature and stress gradients are the steepest. It has also been shown that the thickness and structure of this layer has an important influence on the mechanical properties of injection moulded samples[11,13,14].

In order to study the spatial variation of the orientation distribution in injection moulded polymers we developed a micro-beam pole figure device[15] (*Figure 3*). The micro-beam pole figure attachment was mounted on a Rigaku RU-200B 12 kW rotating anode X-ray generator. The CuK_α radiation was generated at 40 kV and 150 mA using a nickel foil filter. The samples of 0.5 × 0.5 mm square cross-section and about 3 mm in length were cut from injection moulded PEN samples midway between two ends of the samples along the mirror plane with the long axis in the normal direction. These samples were mounted on the goniometer head

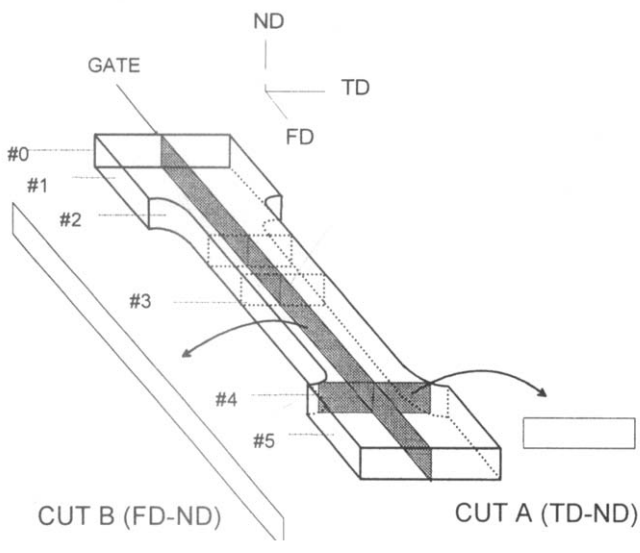

Figure 1 Schematics of the cutting procedures

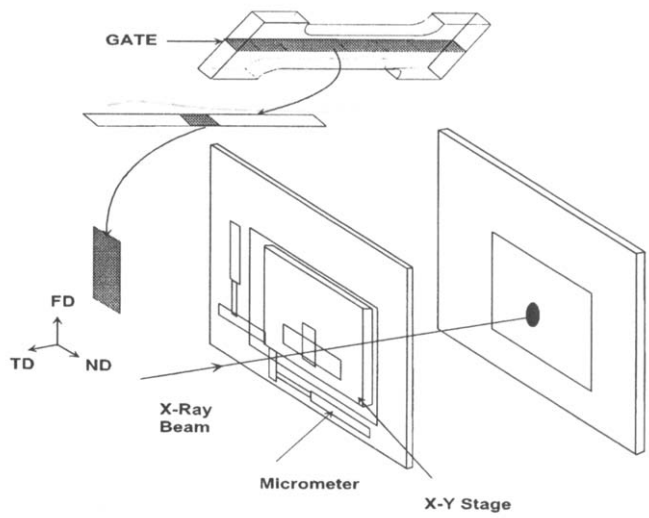

Figure 2 Diagram showing the mounting of the B cut samples to the x–y stage of the micro-beam X-ray camera and the direction of the X-ray beam

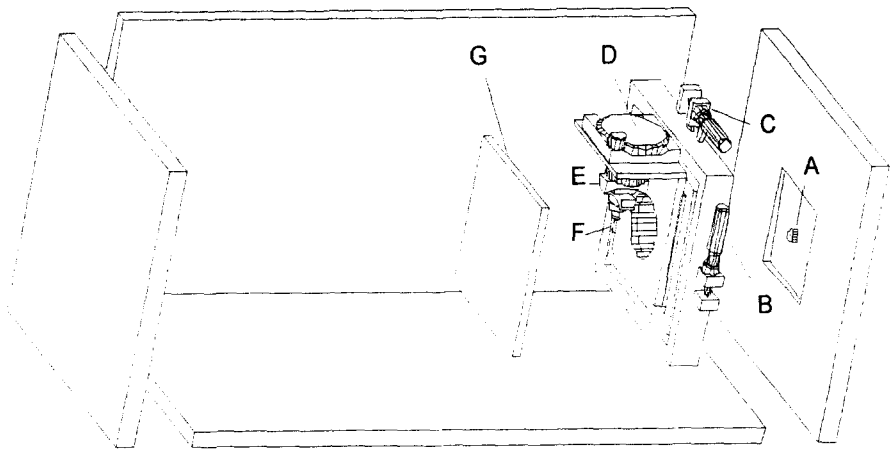

A - Pinhole collimator, B and C – Micrometers (translation on X–Y axes), D – Rotator, E – Goniometer head, F – Sample and G – Film holder

Figure 3 Schematic of micro-beam pole figure device

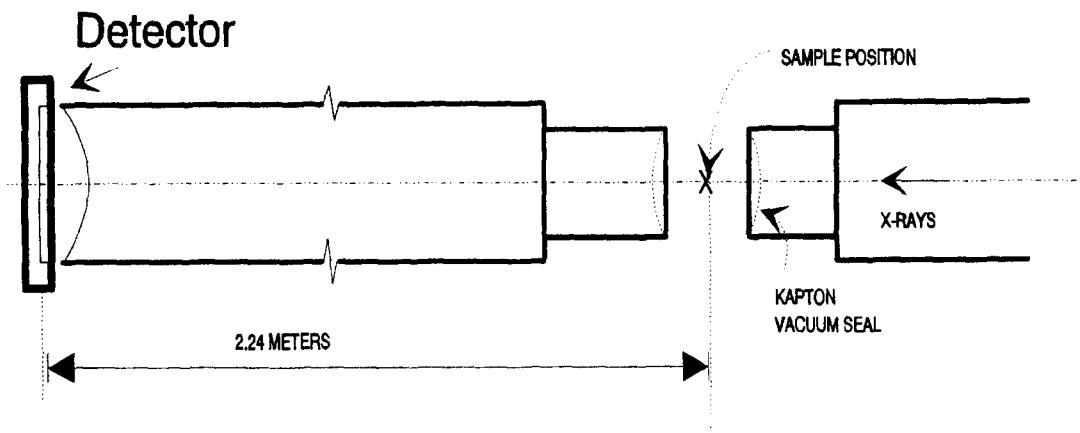

Figure 4 Schematics of the synchrotron beam line used in SAXS study

with their normal direction as the spindle axis. Since this sample contains large spatial variations of orientation, the beam of 100 μm was first aligned with the top surface and WAXS patterns were recorded at angular intervals [$\gamma = 0$ (TD), 15, 30, 40, 50, 60, 70, 80, 85, 90° (FD)]. The sample was then moved axially to align the X-ray beam at a different depth from the surface and the same procedure is repeated. Typical exposure times were 2 h at a sample to film distance of 3.65 cm. The azimuthal intensity distribution of selected diffraction peaks was recorded by digitizing the X-ray films using a 16 bit CCD camera. The pole figures were plotted on the Wulff net using the film procedure. These pole figures were converted to polar net using a coordinate transformation[15].

For comparison, a separate experiment was performed on the automated quarter circle goniometer attachment of the GE XRD-6 generator. A section taken from the shear crystallized region of the PEN sample was mounted on a single crystal orienter with flow direction in the spindle axis. The data were acquired at intervals of 5° in the χ direction (tilt axis) and 10° in the ϕ direction (spindle axis) with an 80 s counting time at each step.

Hot stage WAXS. In order to observe the changes in the phase behaviour of the PEN crystals in the shear

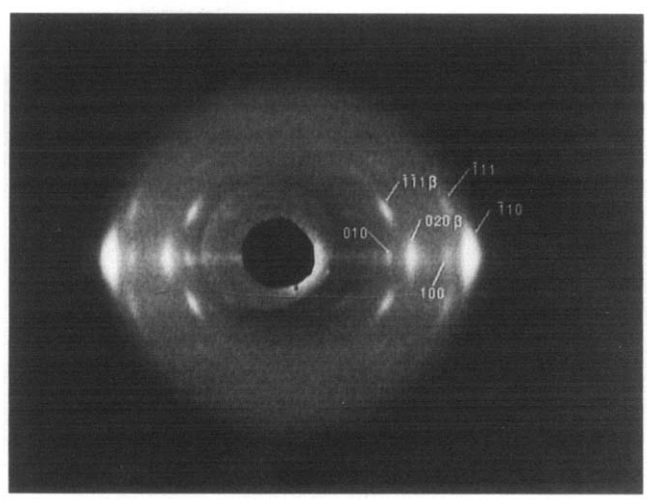

Figure 5 Details of WAXS patterns taken from location No. 3 of a sample moulded at 20°C using the low injection speed. X-ray was directed in the TD

crystallized layer, we used an X-ray hot stage attachment that was developed in our laboratories. The hot stage was mounted on the horizontal X-ray diffractometer. For these experiments the Rigaku RU-200B X-ray generator was operated at 40 kV and 150 mA. The

X-rays were monochromatized using the built in detector side graphite crystal monochromator.

To study the influence of temperature on the WAXS profiles, we chose a step heating method. In this method, a series of diffractometer scans were obtained in transmission mode at 10°C steps from 140–300°C. For each step, the total scanning time was 10 min. The heating rate between two consecutive temperature steps was kept to 5°C min^{-1}.

Small angle X-ray scattering (SAXS)

SAXS patterns of the selected samples were taken at the University of Hamburg DESY Synchrotron Radiation source[16]. The crystalline regions of the B-cuts taken from selected samples were separated and placed in the X-ray beam path connecting the collimated beam to the two-dimensional wire detector (*Figure 4*). The incoming beam was monochromatized to 1.54 Å using a

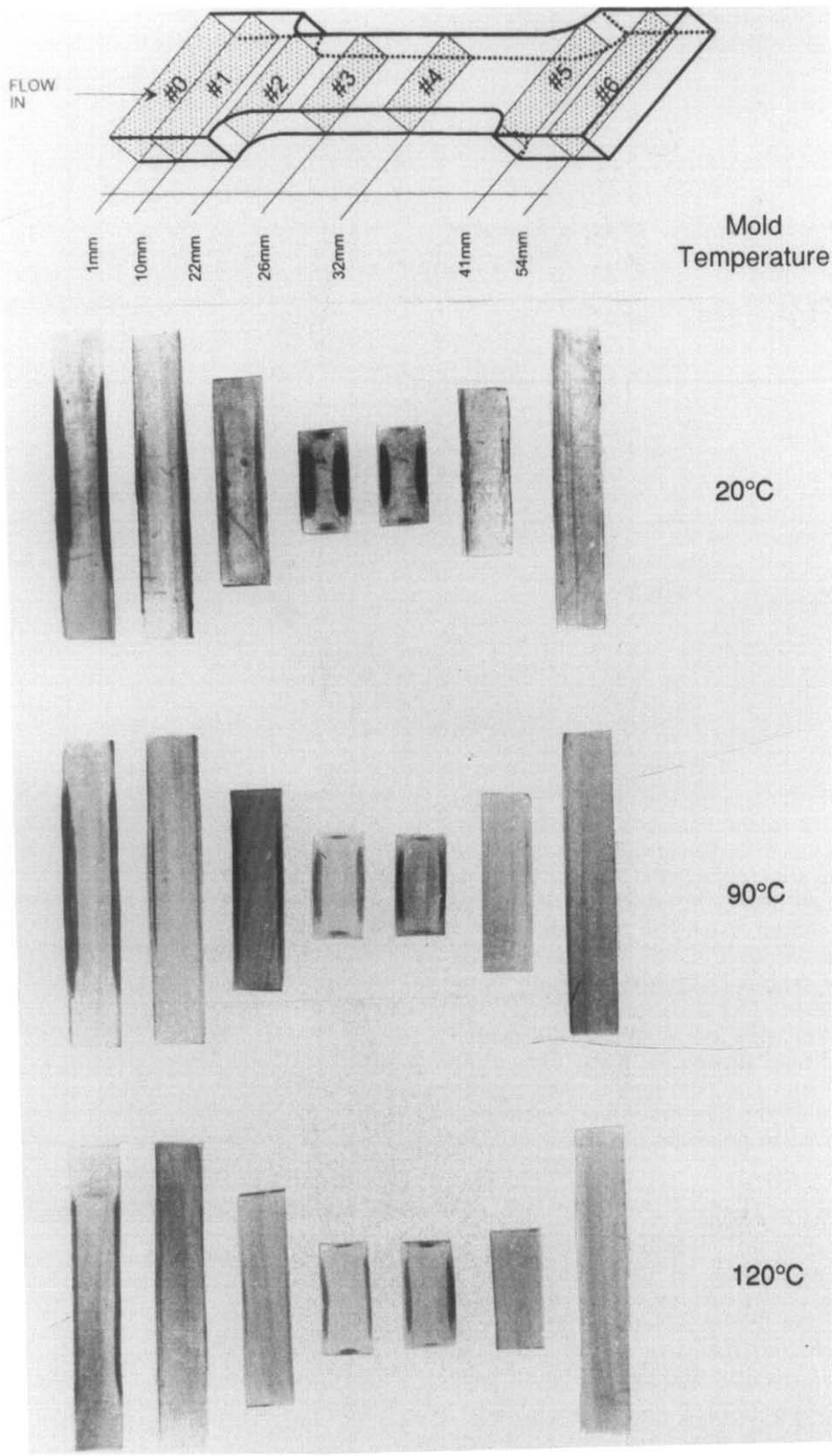

Figure 6 Transmission optical photomicrographs of A cuts taken from the indicated locations of samples moulded using the low injection speed

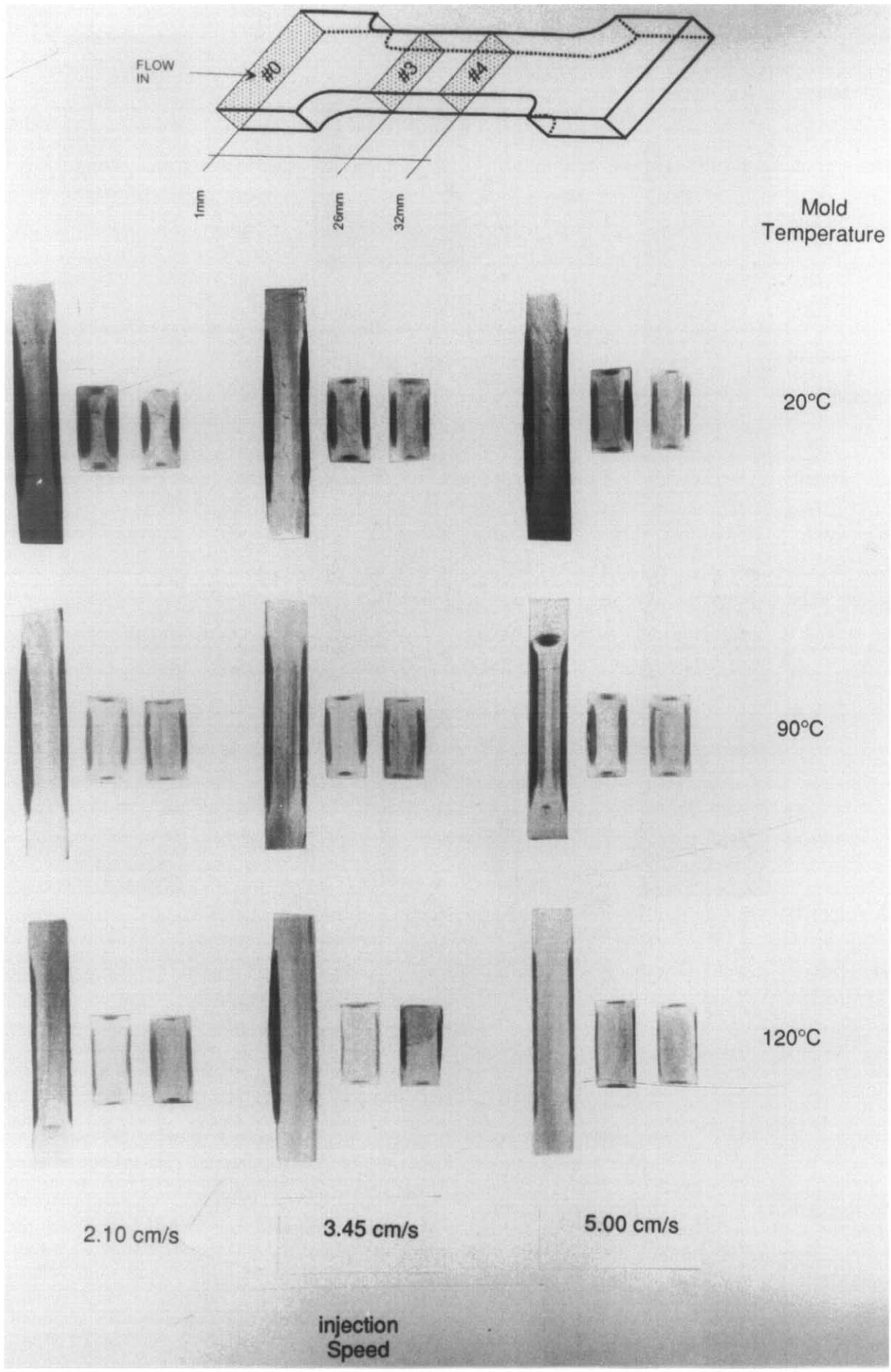

Figure 7 Transmission optical photomicrographs showing the effect of mould temperature and injection speed on the structure of the A cuts taken from the indicated regions

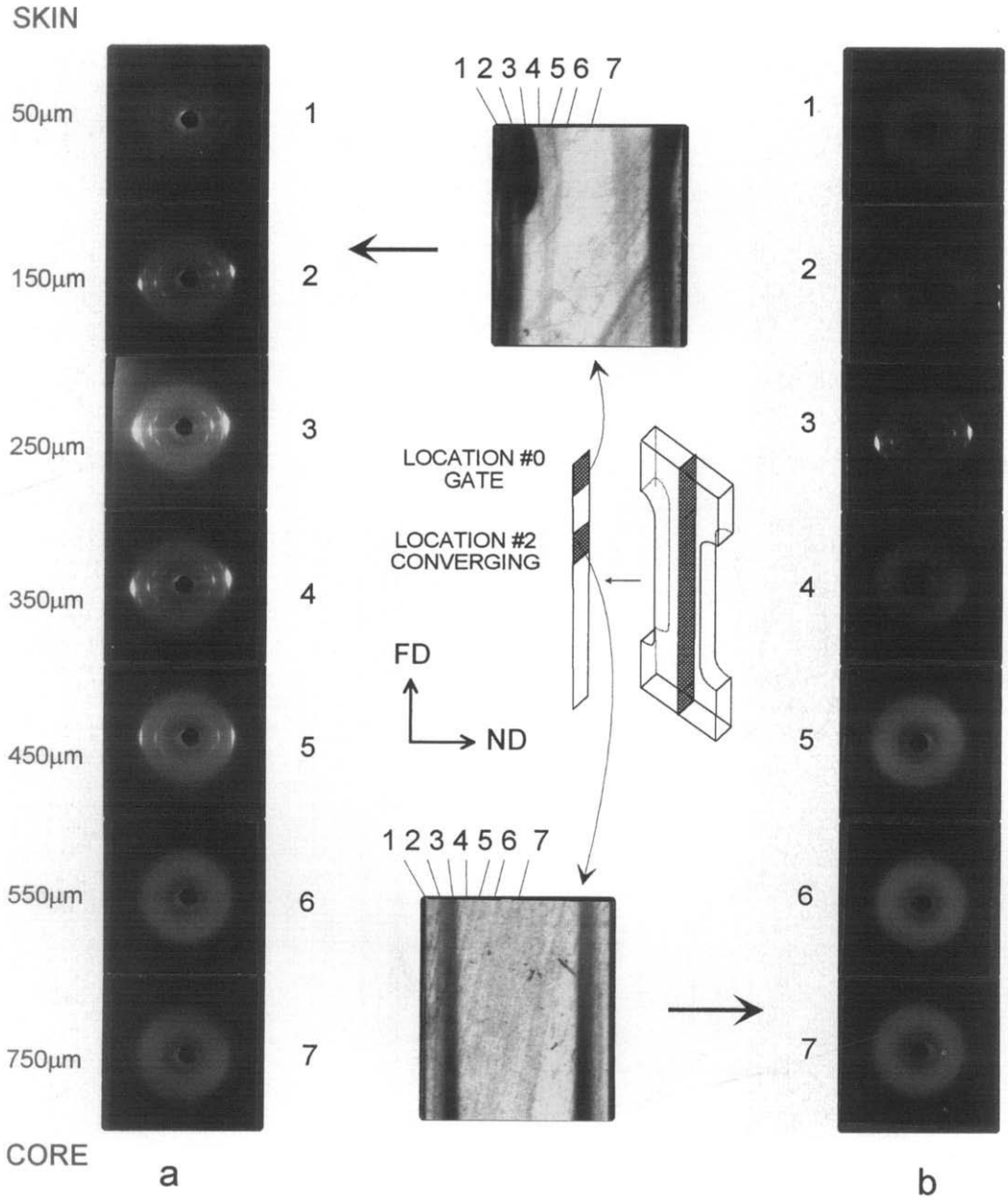

Figure 8 WAXS patterns taken with the MMBX from the locations indicated on the optical photomicrographs of a sample moulded at 20°C using the low injection speed: (a) location No. 0; (b) location No. 2; (c) location No. 3; (d) location No. 5

crystal monochromator. The sample to film distance was 224.5 cm.

RESULTS AND DISCUSSION

Wide angle X-ray diffraction (WAXS)

Identification of WAXS peaks. Before carrying out a detailed analysis of the evolution of the WAXS patterns at different positions of PEN samples, the characteristic peaks belonging to the two crystal forms (α and β) of PEN were identified. *Figure 5* shows typical WAXS diffraction patterns taken from the crystalline regions of samples produced at mould temperatures below the glass transition temperature of PEN. The WAXS patterns of the injection moulded samples presented two distinct features. First, we note that WAXS peaks above the first layer line are either weak or absent indicating the three-dimensional order in this sample is not very good. The other striking feature was the high intensity of the amorphous halo at the background. In this figure, the presence of both strong α-form ($\bar{1}\,1\,0$), (1 0 0), (0 1 0), ($\bar{1}\,1\,1$) and β-form (0 2 0) and ($\bar{1}\,\bar{1}\,1$) diffraction spots indicate both phases coexist in this region and each phase is quite highly oriented. The diffraction peaks corresponding to the α-form of PEN were indexed according to the crystal structure published by Mencik[3]. The β-form planes on the other hand, were indexed according to the d-spacing values calculated from the unit cell dimension that was reported by Buchner *et al.*[2]. However, there were two peaks at the respective 2θ angles of 16.02° and 42.90° that could not be indexed. The latter peak was also observed by Cakmak and Kim[4] upon annealing melt spun fibres that showed the presence of β crystals. These peaks may be associated with the β-form whose detailed crystallographic analysis is currently lacking.

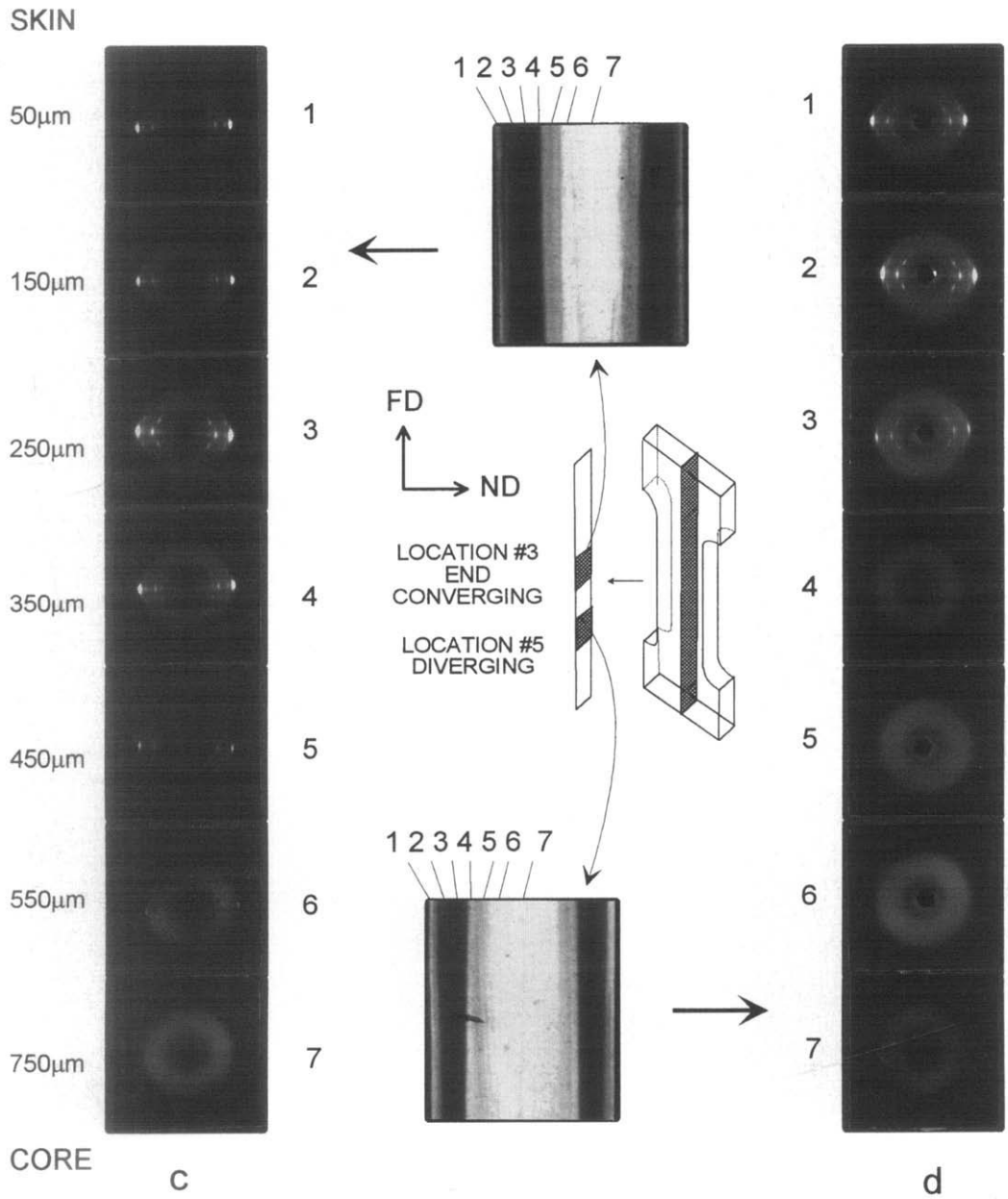

Figure 8 (*Continued*)

Earlier research conducted in our group[8,9] showed that PEN crystallizes exclusively in the α-form at temperatures below 220°C and $\alpha + \beta$ mixture occurs in the temperature range 220–240°C and above 240°C β-form occurs exclusively. It was also reported that the β-form can be preferentially grown when PEN is subjected to high deformation fields such as extensional fields generated along the melt spin line[9]. This indicates that the shear crystallized layers in injection moulded samples should be formed under significant stress in the temperature range 220–250°C.

WAXS patterns by MMBX. In our previous paper[10] we have shown that, when moulded below or around its glass transition temperature ($T_g = 120$°C) PEN exhibits an amorphous skin–crystalline intermediate–amorphous core type internal structure. *Figures 6* and *7* show that mould geometry, injection speed and mould temperature are the main variables, which play an important role in the evolution of the details of the structural gradients. The stress induced crystalline layers are prominent at mould locations where converging flows have taken place (*Figure 6*, Location Nos. 0, 3 and 4). These results also showed that although the thickness of the crystalline layers at a given location decreased with increasing mould temperature and injection speed (*Figure 7*), the essential features of the three layer structure are preserved along the flow direction.

To study the crystallinity and orientation levels in the gapwise (ND) direction, samples were cut using Procedure B. We then took a series of WAXS patterns with 100 μm intervals from skin to core. As shown in *Figure 2*, the X-ray beam was directed along the TD normal to the FD and ND plane. *Figure 8* shows such WAXS patterns taken from different locations of a sample moulded at 20°C using the low injection speed along with the transmission optical photomicrographs of the same locations. In these patterns the vertical direction is the flow direction and the horizontal direction is the normal direction. We observe that the

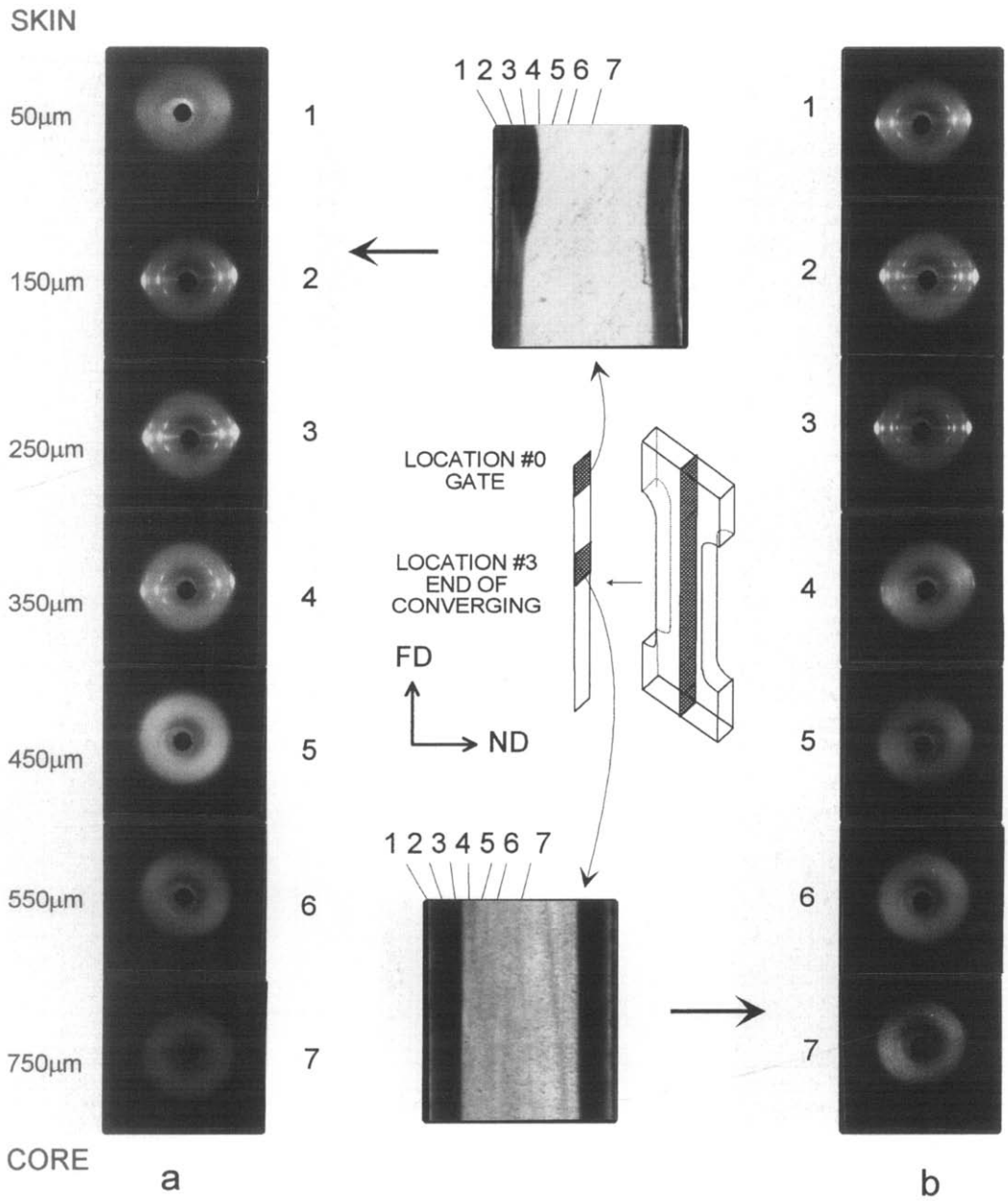

Figure 9 WAXS patterns taken using the MMBX camera at the indicated positions on the optical photomicrographs of location (a) No. 0 and (b) No. 3. Sample moulded at 90°C using the low injection speed

dark shear layers are characterized by highly oriented crystalline diffraction spots, whereas the transparent core is characterized by an amorphous halo. In our earlier optical measurements[10], we found that with the exception of the No. 2 location the skin layer is very thin (~30–60 μm) and with our beam size of 100 μm we could not detect it separately. However, the relative thickness of the crystalline shear and amorphous core region can be estimated by comparing the regions where diffraction spots and amorphous halo are observed. From the optical photomicrographs, we can see that there is a good correlation between the optically visible thickness of the crystalline layers (dark opaque layers) and that measured by the X-ray (the region over which the crystalline peaks are observed). Of course, this correlation is limited by the resolution of the X-ray beam diameter. The sharp diffraction peaks in the shear crystallized regions and their orientation indicates that the chains are oriented primarily in the flow direction.

We also note that the transition from the crystalline layers to the amorphous core is rather abrupt and occurs almost without loss of orientation. This can also be seen in the optical photomicrographs: there is a sharp boundary between the dark crystalline layers and transparent amorphous core. This boundary marks the time of cesssation of flow during the filling stage. During the flow there is a high shear stress zone between the solid boundary and the flowing melt that moves towards the core, as a result of cooling and/or crystallization. Stress induced crystallization takes place at this zone, where the polymer chains are subjected to large deformation gradient with the local velocities being zero in the solidified region and maximum at the core. When the melt stops flowing, the main driving force for crystallization in the solidifying front is mostly eliminated due to rapid decay of stresses. After this point, the structure formation begins to be governed by thermal crystallization kinetics. In this polymer, crystallization in

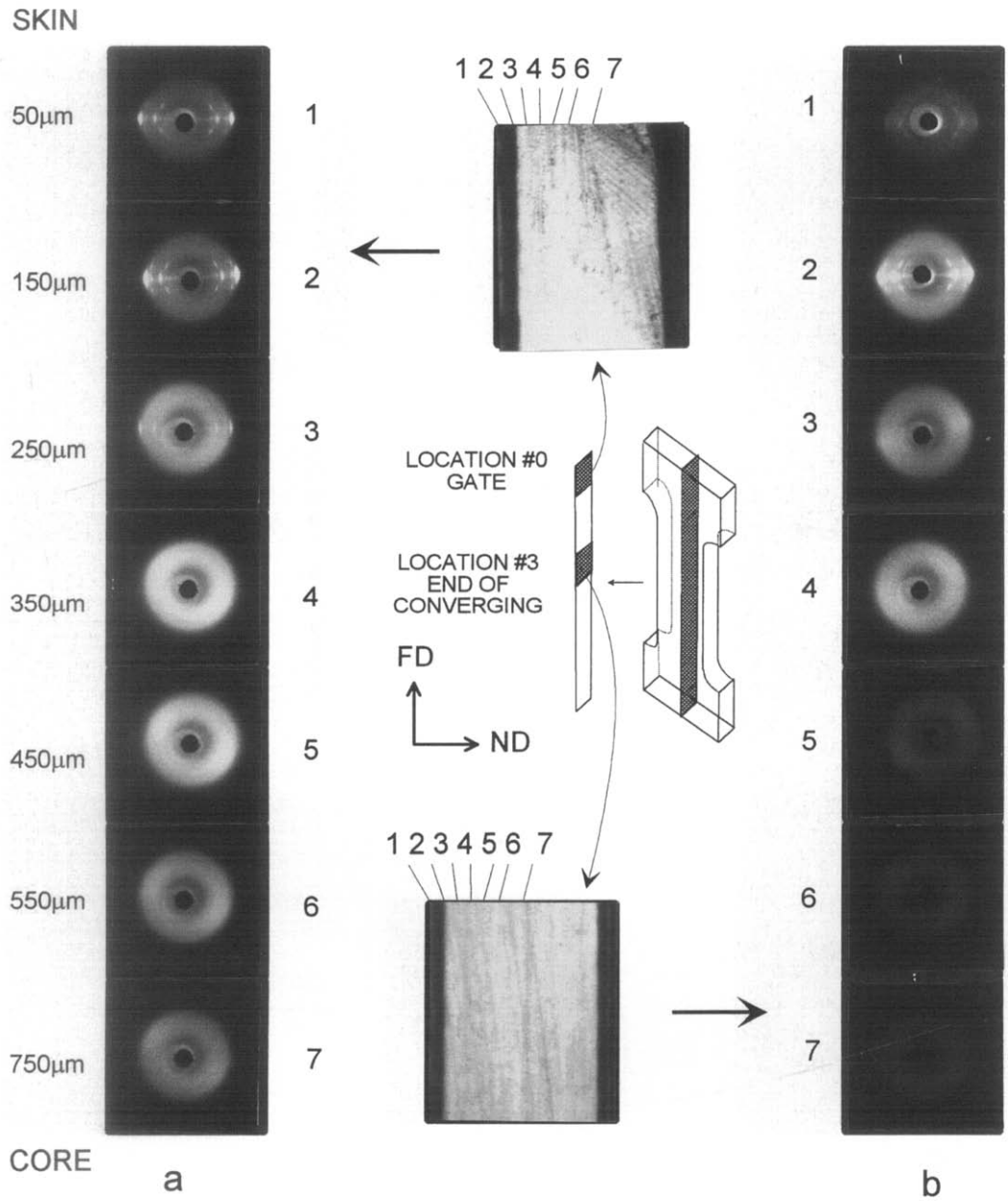

Figure 10 WAXS patterns taken using the MMBX camera at the indicated positions on the optical photomicrographs of location (a) No. 0 and (b) No. 3. Sample moulded at 120°C using the low injection speed

the absence of stress is quite slow and, as a result, the interiors of the samples vitrify under the experienced cooling conditions.

Even at locations No. 2 (*Figure 8b*) and No. 5 (*Figure 8d*), which mark the beginning and end of shear crystallized layers along the flow direction (cf. *Figure 6*), there remains a significant level of orientation in the crystalline layer. This indicates that the level of orientation is not only conserved in the gapwise (ND) direction but also at different locations along the flow direction. At the gate (*Figure 8a*) and converging regions of the sample moulded at 20°C (*Figure 8b*), the tilting of the local symmetry axis towards the outer surface is observed (for example see the pattern taken at 250 μm from the surface). In either case the tilting was no more than 6.5°. No tilting was observed at locations Nos. 3 and 5. These observations confirm that the crystallization occurs only when PEN is oriented. As expected from the optical photomicrographs (*Figures 6* and 7), the maximum degree of crystallization is at the Nos. 0 and 3 locations where the stress effects are at a maximum. While the polymer melt goes through the converging regions (and No. 3 locations) during the filling stage, it experiences elongational stresses along with shear (due to acceleration of polymer melt while entering the narrower section). The elongational stresses being more effective in accelerating the stress induced crystallization[17] the material exhibits higher crystallinity and thicker crystalline layers at these locations. The location No. 0 is located just downstream of the runners and gates where significant shearing is experienced by the polymer chains before entering the cavity. This also causes increases in thickness of the shear crystallized layers.

As we mentioned earlier, the increase of mould temperature from 20 to 120°C mainly results in structural changes in the thickness direction with minimal changes observable along the flow direction (*Figure 6*). Therefore, we chose locations Nos. 0 and 3 to investigate the

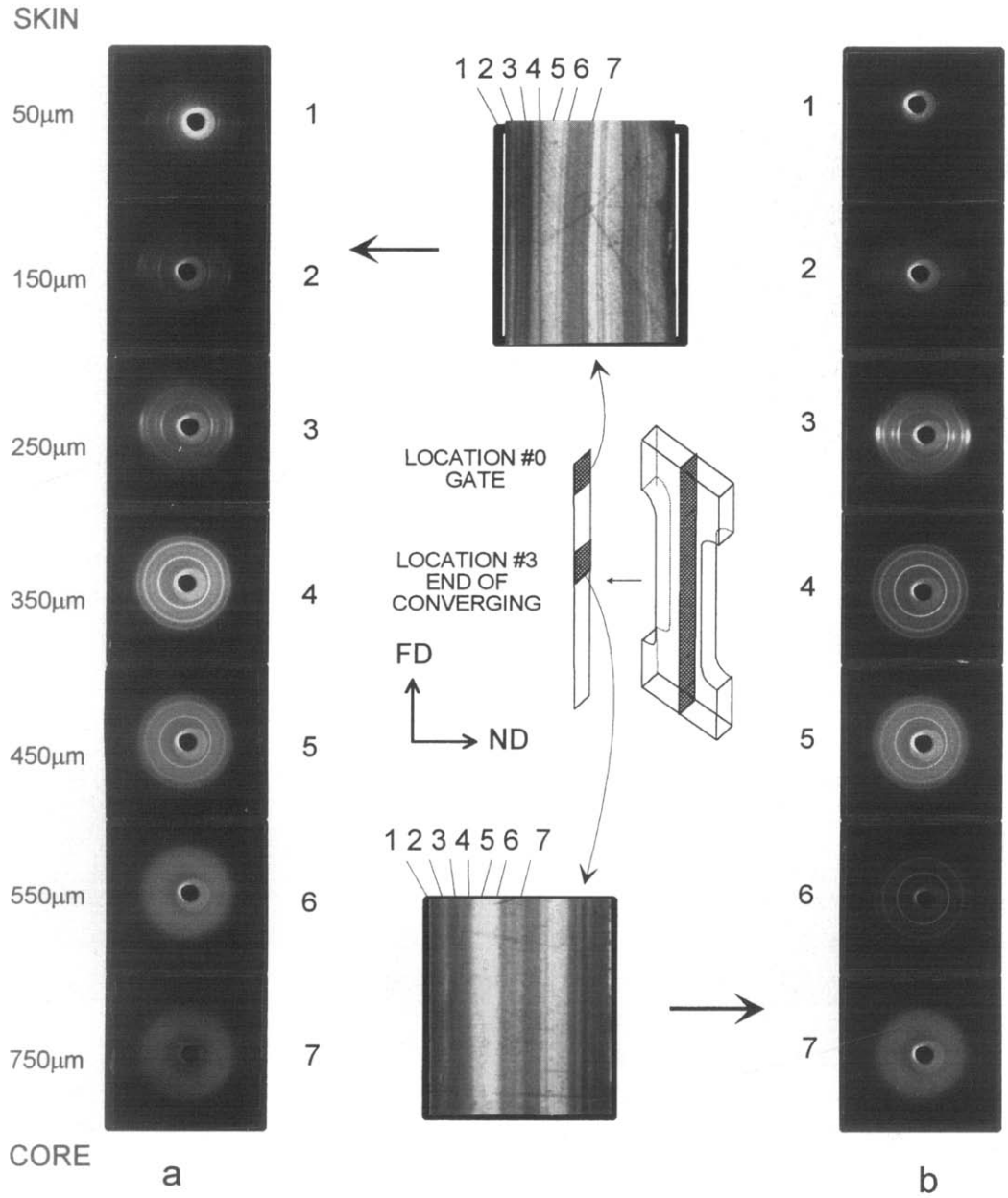

Figure 11 WAXS patterns taken using the MMBX camera at the indicated positions on the optical photomicrographs of location (a) No. 0 and (b) No. 3. Sample moulded at 180°C using the high injection speed. Holding time = 10 min

processing condition effects on the development of crystallinity and orientation. *Figures 9* and *10* show WAXS patterns taken from Nos. 0 and 3 locations of samples moulded at 90 and 120°C respectively. As expected, among these two locations the crystallinity of the location No. 3 is higher due to the increase of fraction of elongational flow component in this shear dominated flow field. We can see that the effect of increasing the mould temperature is to reduce the thickness of the shear crystallized region while preserving the high level of orientation. The decrease in the thickness of the shear crystallized regions was attributed to the decrease in the stress history of the polymer melt with increasing mould temperature[10]. The existence of high levels of orientation indicates that, although the magnitude of the deformation field that is experienced by the polymers at the solid–melt interface during filling is similar to low mould temperatures, it is confined to small regions near the skin at elevated mould temperatures.

When the mould temperature is set at about 150°C and higher, the thermally activated crystallization also starts to play a role in the formation of structural gradients. This is demonstrated in *Figure 11* where the micro-beam WAXS data taken from a sample moulded at 180°C and held in the mould for 10 min are shown. This figure also includes the transmission optical photomicrographs of the samples where these WAXS patterns were obtained. These data indicate that the PEN crystals having high orientation levels generally concentrate in the first 250 μm from the surface. Contrary to what we observed at low mould temperatures, at 180°C, the regions near the core (350–450 μm) becomes crystalline without any evidence of orientation. This indicates that the thermally induced crystallization begins to dominate the structure formation in these regions. At 500 and 750 μm the gate region is still amorphous, however, due to the decrease of cross-sectional area in No. 3 location the thermally induced crystallization has advanced deeper towards the

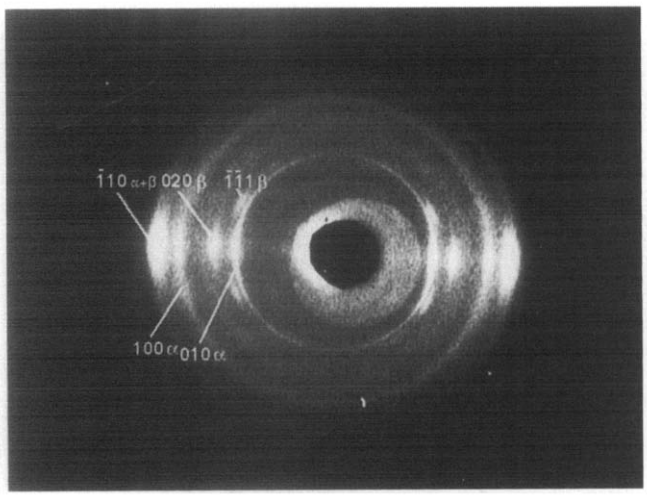

Figure 12 Details of the WAXD patterns taken from location No. 3 of a sample moulded at 180°C using the high injection speed. Holding time = 10 min, distance from skin = 250 μm

core. Qualitative observations of these patterns indicate that the orientation levels decrease from skin towards the core, and the overall orientation levels observed in these samples are generally much lower than those observed at low mould temperatures (*Figures 7–9*).

If we examine the details of the WAXS patterns, such as the one obtained at 250 μm from the surface at No. 3 location of *Figure 11* as shown in *Figure 12*, we observe that there are two sets of patterns superimposed. Diffraction peaks belonging to the first set are rather sharp and both α and β peaks are present, indicating that crystallization has occurred in the 220–250°C range, during the filling stage. We also see a second set of diffraction rings superimposed onto the first set of highly oriented arcs. Note that the diffraction spots formed during filling and belonging to β crystalline form do not have any second set of rings superimposed on them suggesting that the structural formation in these regions is a two step process. First, oriented shear crystallized layers containing both α and β crystalline regions are formed during the filling stage. In the subsequent holding stage the stresses developed during filling rapidly decay.

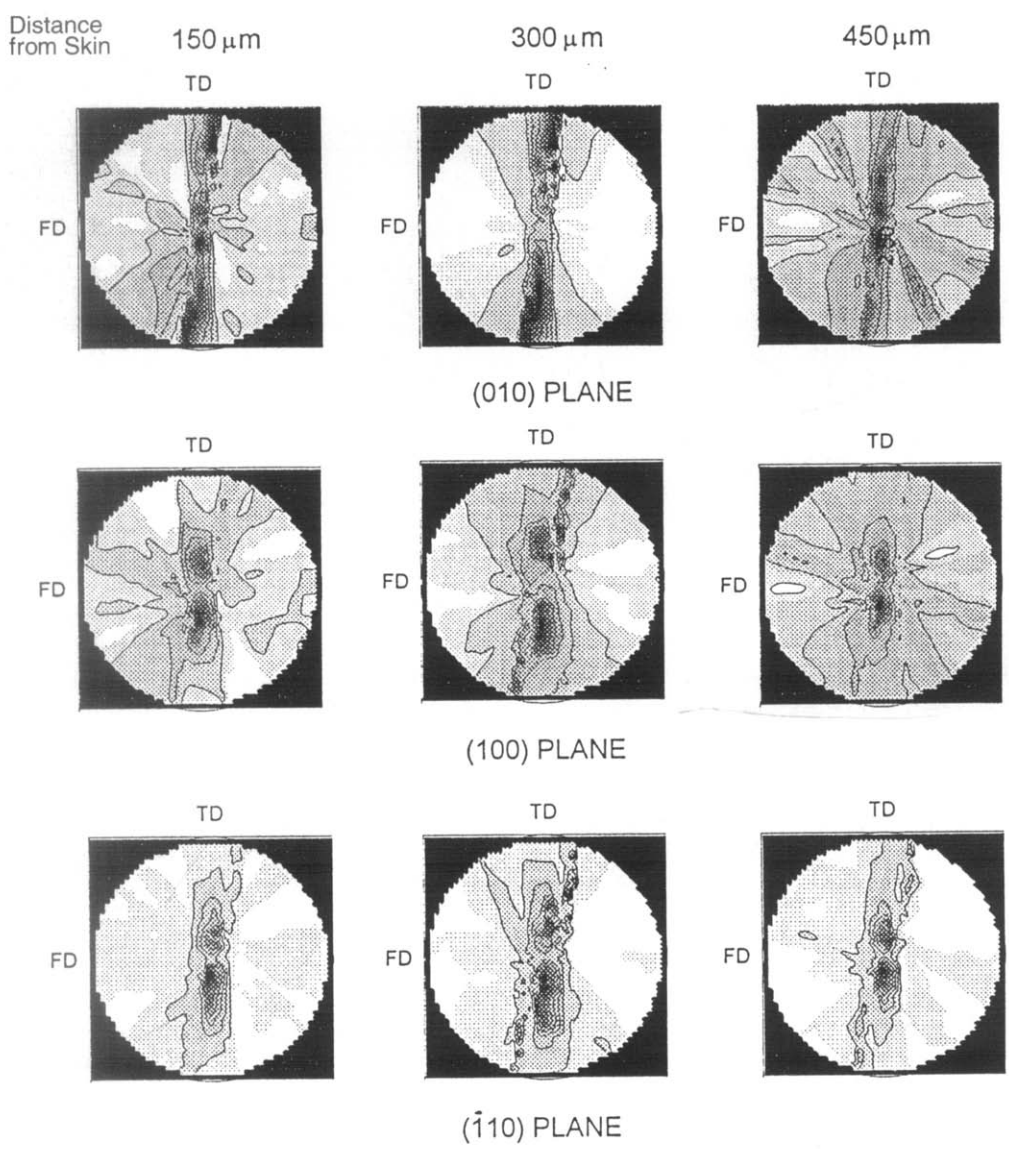

Figure 13 Contour plots of the pole figures of ($\bar{1}$ 1 0), (1 0 0) and (0 1 0) planes of α crystal form. PEN injection moulded at 20°C using the low injection speed, location No. 3

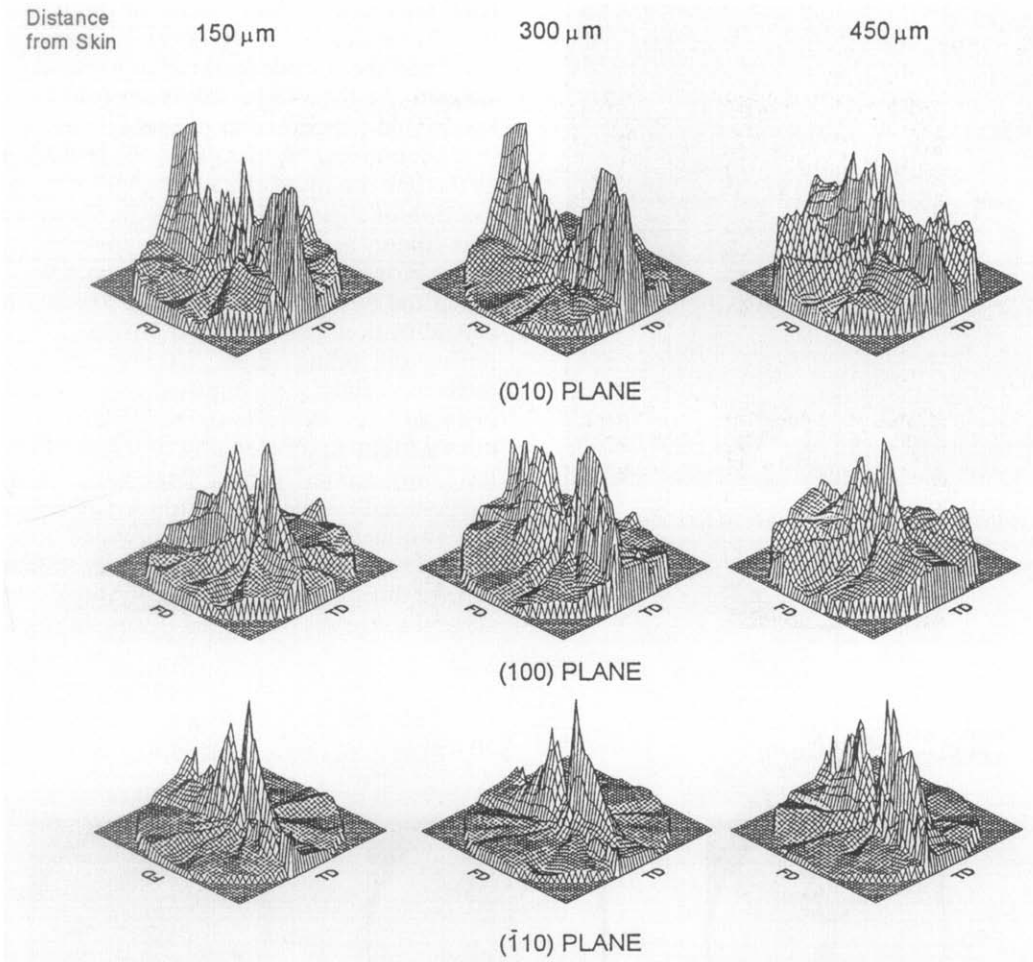

Figure 14 Surface plots of the pole figures of ($\bar{1}$ 1 0), (1 0 0) and (0 1 0) planes of α crystal form. PEN injection moulded at 20°C using the low injection speed, location No. 3

Since the heat loss at the polymer-mould boundary becomes rather slow at this high mould temperature, the second crystalline population crystallizes thermally in a quiescent state and as a result, exhibit random orientation. What is most interesting, in the above WAXS pattern, is that 180°C being lower than the minimum formation temperature for the β crystals[9], randomly oriented crystals of the β-form do not grow during the holding stage. As a result, no circular ring is superimposed on the highly oriented patterns of (0 2 0), ($\bar{1}$ 1 0) and ($\bar{1}$ $\bar{1}$ 1) planes of β-phase, that formed during the filling stage due to stress induced crystallization.

Preferential orientation in crystalline regions. In order to investigate spatial variation of orientation distribution in the crystalline region in injection moulded samples, we selected a sample moulded at 20°C with low injection speed. A sample for the pole figure study was cut from the No. 3 location. The MMBX WAXS experiments of the previous section showed that the thickness of shear crystallized layer at this location was 450 μm. Considering the resolution of the microcamera (100 μm) three pole figure sets at 150, 300 and 450 μm distance from the skin were prepared. *Figures 13–15* show the resulting pole figures.

Figures 13 and *14* show the WAXS pole figures on (0 1 0), (1 0 0) and ($\bar{1}$ 1 0) planes of the α phase for three different distances from the surface. As indicated earlier these pole figures (*Figures 13–15*) were constructed from the digitized images of the WAXS film patterns taken at a series of rotation angles about ND. For quantitative orientation determination a separate experiment with a diffractometer was performed and will be discussed below (*Figure 16*).

The data are presented in equiangular projection isointensity contour graph form (*Figure 13*) as well as in three-dimensional form (*Figure 14*) in order to ascertain the details of the orientation behaviour in these shear layers. The basic orientation behaviour at these three different layers are very similar: The ($\bar{1}$ 1 0) poles are primarily oriented in the normal direction (the centre of the pole figures) with a fair degree of distribution towards the transverse direction. It should be noted that the centre of the pole figure does not contain a data point due to the plotting procedures and artificially appear low in intensity. The relative positions of the intensity maxima are not completely independent and related to one another through unit cell geometry. The poles of (0 1 0) plane are concentrated in the transverse direction with a fair level of spread towards the normal direction. The intensity distribution of all three plane poles are confined in a very narrow band in the ND–TD plane indicating substantial chain orientation parallel to the FD.

The (0 2 0) and ($\bar{1}$ 1 0) planes of the β-form show the same orientation mode as the α-form. As expected from the MMBX WAXS results, this orientation is preserved throughout the crystalline region, although there is a slight

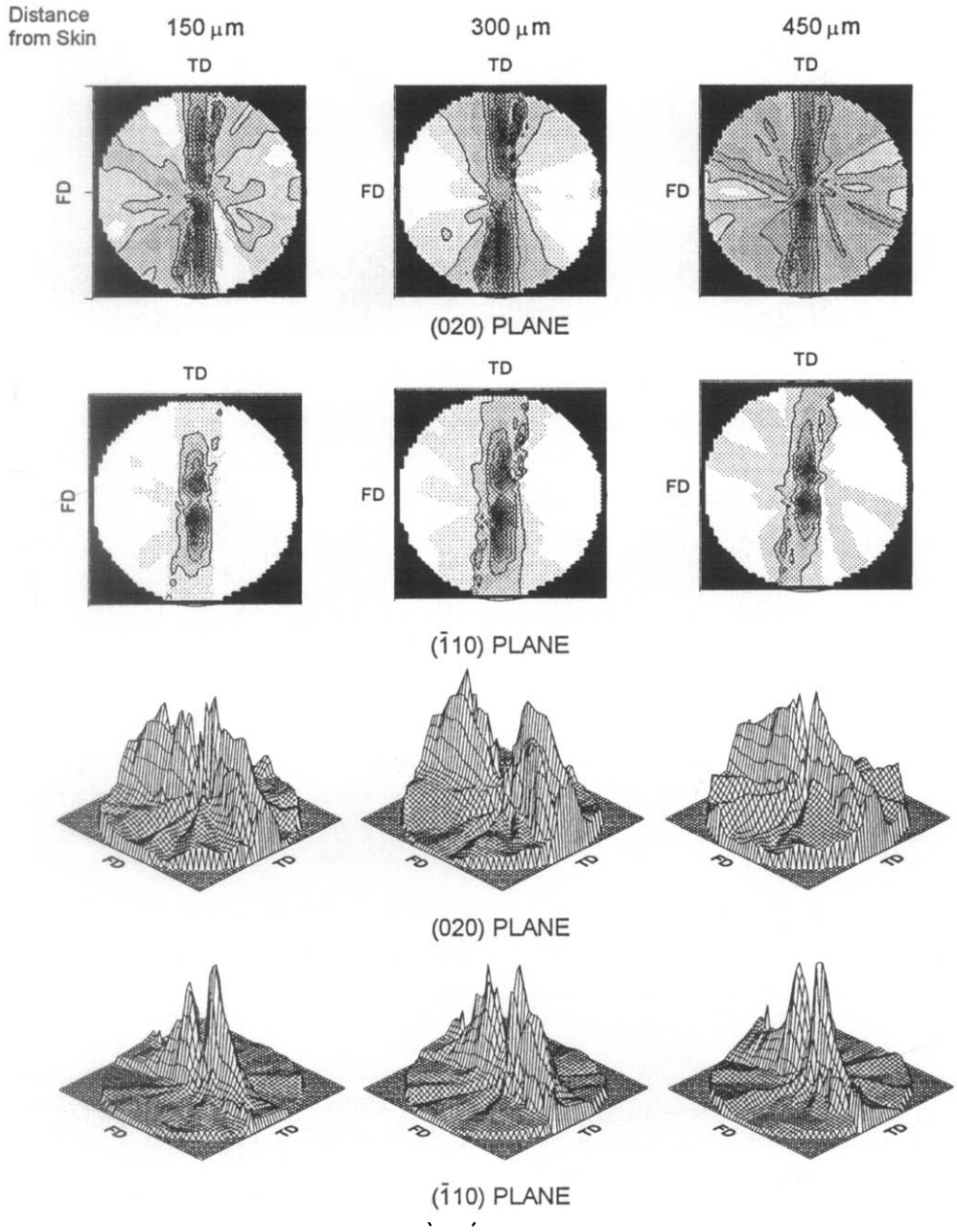

Figure 15 Contour and surface plots of the pole figures of (0 2 0) and ($\bar{1}$ 1 0) planes of β crystal form. PEN injection moulded at 20°C using the low injection speed, location No. 3

decrease in sharpness of the intensity profiles towards the core indicating decrease of preferential orientation.

The above discussions on the pole figures derived from WAXS film patterns help us examine the relative differences between various positions in the moulded parts. This is due to the nature of the X-ray films whose sensitivities to broad range of intensities is limited compared to diffractometer or other detector systems.

Once it was determined from the micro-WAXS pole figure technique that the orientation levels in the shear crystallized regions does not change significantly from position to position, we then prepared a larger sample covering the full thickness of the shear crystallized region for examination with the pole-figure diffractometer technique. The pole figures of the (0 1 0) and ($\bar{1}$ 1 0) planes of the α-form were prepared using a quarter circle GE diffractometer. The pole figures for the (1 0 0) planes could not be obtained since their intensity was too low to be detected. The resulting pole figures are displayed in *Figure 16a*. A comparison of *Figure 16a* to *Figures 13–15* shows that there is a good agreement between the pole figures obtained using the two methods. However, as a result of the averaging of the orientation of the whole crystalline region, the pole figures obtained through the diffractometer indicate distribution of orientation of poles of ($\bar{1}$ 1 0) planes in ND–TD plane with substantial concentration of the intensity in the normal direction.

The data obtained through the GE quarter circle goniometer was used to determine the White–Spruiell biaxial orientation factors[18] of the chain axis and the ($\bar{1}$ 1 0) planes. The second moment of orientation of the chain axis, $\langle \cos^2 \phi \rangle_c$ was determined by applying the Wilchinsky's rule[19] to the pseudo-orthorhombic unit cell proposed by Lee and Cakmak[8]:

$$\langle \cos^2 \phi_{c,Z} \rangle = 1 - 0.844 \langle \cos^2 \phi_{\bar{1}10,Z} \rangle - 1.156 \langle \cos^2 \phi_{010,Z} \rangle \quad (1)$$

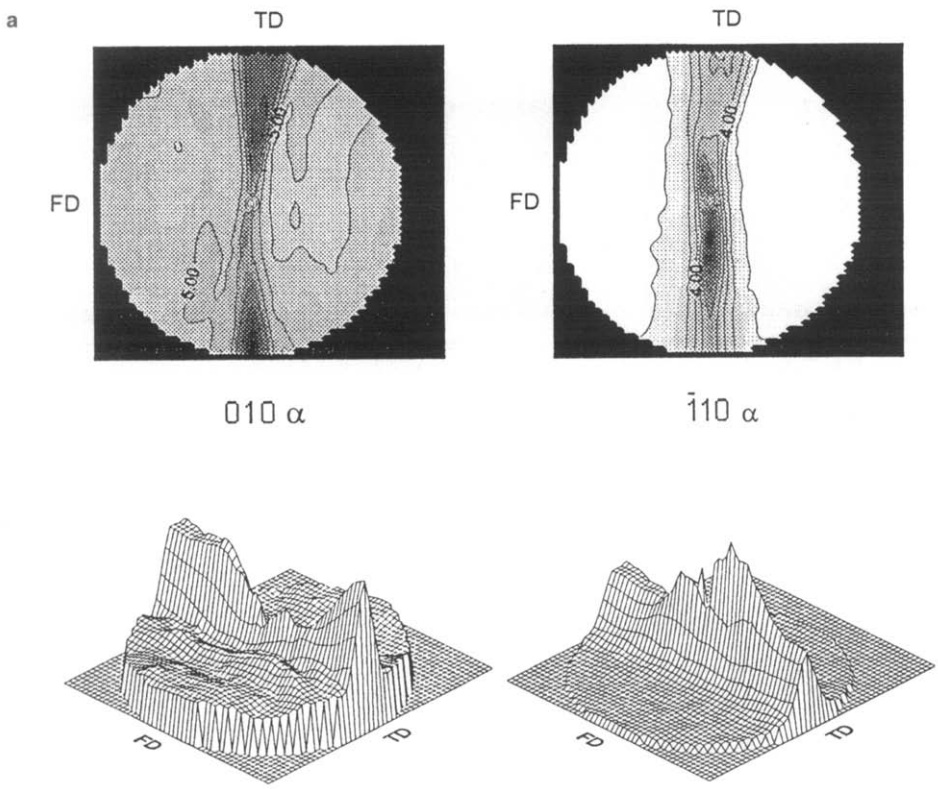

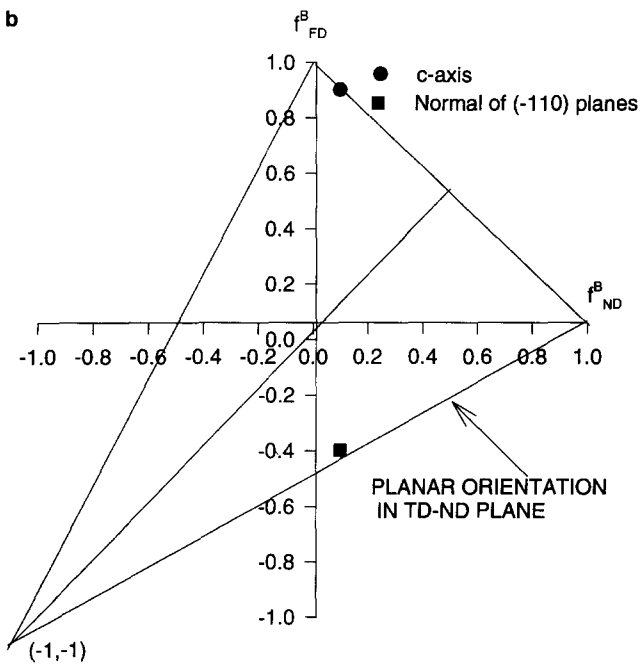

Figure 16 (a) Contour and surface plots of the pole figures of (0 1 0) and ($\bar{1}$ 1 0) planes of crystalline region of injection moulded PEN. (b) Biaxial orientation factors for *c*-axes and the poles of ($\bar{1}$ 1 0) planes which are nearly normal to the naphthalene planes in the chain backbone

The biaxial orientation factors

$$f^B_{i,FD} = 2\langle\cos^2\phi\rangle_{i,FD} + \langle\cos^2\phi\rangle_{i,ND} - 1$$
$$f^B_{i,ND} = 2\langle\cos^2\phi\rangle_{i,ND} + \langle\cos^2\phi\rangle_{i,FD} - 1 \quad (2)$$

of the *c*-axis and ($\bar{1}$ 1 0) plane of the α-form were calculated as

$$f^B_{c,FD} = 0.9 \qquad f^B_{c,ND} = 0.1$$
$$f^B_{\bar{1}10,FD} = -0.4 \qquad f^B_{\bar{1}10,ND} = 0.1$$

The *c*-axes are very highly oriented along the flow direction. The ($\bar{4}$ 3 0) planes that are parallel to the plane of naphthalene molecules makes an angle of 7.7° with the ($\bar{1}$ 1 0) planes[3]. Since the normals of the ($\bar{1}$ 1 0) planes exhibit planar orientation in the TD–ND plane (*Figure 16b*), the texture of these regions is *in between* transverse isotropy and uniplanar-axial texture ($\bar{4}$ 3 0) [0 0 1] where the *c*-axis is parallel to the flow direction with ($\bar{4}$ 3 0) planes roughly parallel to the broad surface of the moulded sample. This behaviour is quantitatively shown in biaxial orientation factor triangle in *Figure 16b*.

High temperature WAXS. The thermal analysis and hot stage microscopy studies of the shear crystallized regions[10] showed the presence of a crystal population whose melting temperature (301°C) is 30°C higher than the melting temperature of PEN (270°C) in this region (*Figure 17*). This observation suggested the existence of a new crystal form or a population of more perfect crystals in these regions. On the other hand, the analysis of the WAXS patterns showed that both α and β crystals were present in the shear crystallized regions. Since the thermal behaviour of the two forms are similar[5,9] we could not determine which form is responsible for this phenomenon by sole means of thermal characterization. In order to clarify the details of this unusual formation, we conducted a hot stage WAXS experiment where the intensity of the diffraction peaks belonging to different crystal forms were followed as the sample is heated. In order to eliminate the orientation effects on the relative

intensity of the peaks, the shear crystallized layers cut out from a sample moulded at 20°C using the low injection speed were crushed into powder form. The powdered PEN crystals were sandwiched between beryllium plates that were subsequently placed in the hot stage.

Equatorial transmission WAXS scans taken during heating steps are shown in *Figure 18*. The initial scan taken at 35°C showed broad peaks due to the low overall crystallinity in the shear regions. After the sample reached the glass transition temperature, PEN slowly started to crystallize as indicated by the increase in the intensity of the major diffraction peaks. Around 200°C the crystallinity was high enough to index the major peaks. We noted that the intensity of the α peaks continued increasing after 200°C and reached a maximum around 240°C. The intensity of β peaks on the other hand, remained constant during this stage. The same behaviour was observed earlier by Zachmann *et al.*[5] and Cakmak and Kim[9] and was attributed to the fact that β crystals can only grow when the crystallization temperature is above 240°C. The intensity of both α and β peaks reaches a maximum at the initial stage of crystallization. Cakmak and Kim[9] also observed this phenomenon in the annealed PEN fibres: As spun fibres showed distinct β peaks only at take up speeds around 3500 m min^{-1}. On the other hand, the fibres that were spun at take up speeds in the range 1500–3500 m min^{-1} had very low crystallinity and did not show distinct diffraction peaks. After annealing at 220°C, both α and β peaks became visible in these samples.

The melting that starts around 260°C becomes noticeable at 270°C by a marked decrease in the intensity of the α peaks. They disappear at 290°C while the (0 2 0) and ($\bar{1}$ $\bar{1}$ 1) peaks of the β-form remain visible. With further increase in temperature, these β peaks disappear around 300°C. In an earlier research on fibre spinning of PEN, we also observed a significant increase in melting temperature at high take up speeds which also accompanies increases in fraction of β form. This indicates that the β crystalline phase has a higher melting point as compared to the α.

This was also supported by our hot stage optical microscopy results[10] which show the remnants of highly birefringent threads at temperatures (270–300°C) where only the β form crystalline peaks were.

SAXS

In the previous section we observed that in the WAXS patterns of PEN diffraction peaks above the first layer line were uniformly absent indicating relatively poor registry between the chains along their chain axes. In addition, the SAXS patterns obtained from the shear crystallized regions of the sample moulded at 20°C (*Figure 19a*) indicates the absence of discrete scattering patterns both in the FD–ND and FD–TD plane. This suggests that the periodic variations of electron density associated with alternating crystalline and amorphous regions are absent in these regions. Moreover, this result suggests that the thread-like birefringent precursors observed during the hot stage optical microscopy are aggregates of extended crystalline regions that do not show a regular periodicity in the flow direction. This, however, does not mean the absence of disordered regions but it means that the spatial correlation between these regions are absent in the shear crystallized layers.

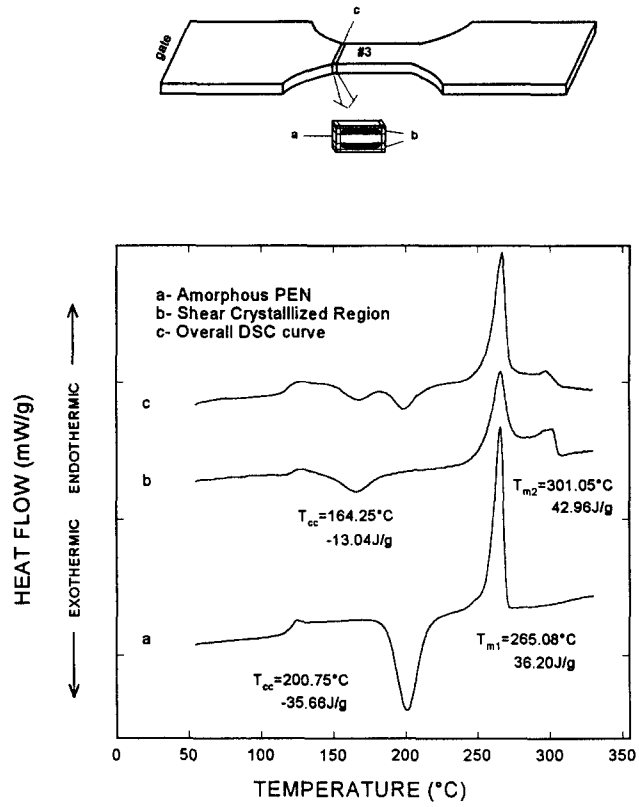

Figure 17 D.s.c. scans: (a) of the amorphous skin and core regions cut from the same sample using Procedure C; (b) of the crystalline region cut from the same sample using Procedure C; and (c) of the A cut taken from location No. 3. Sample moulded at 20°C using low injection speed

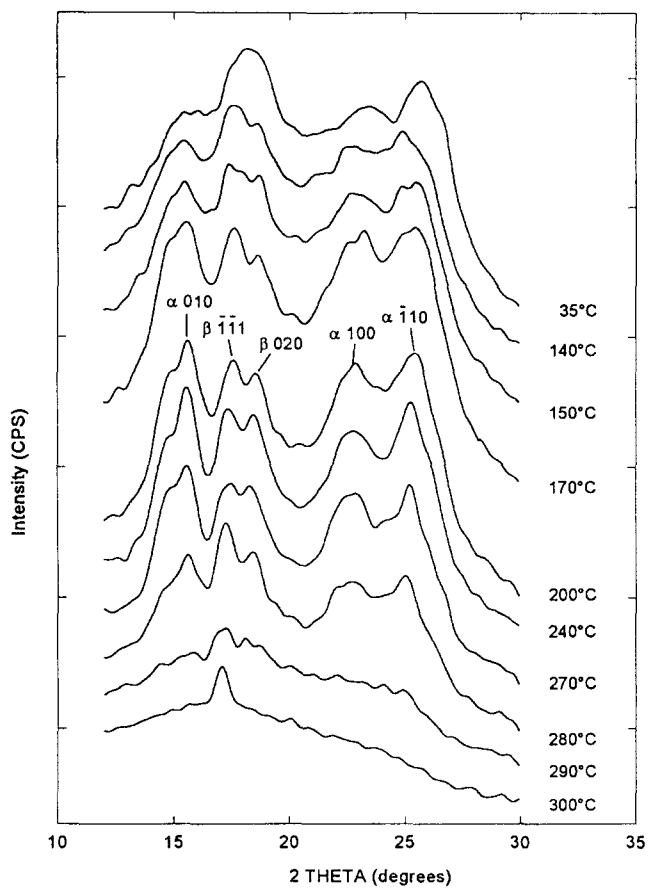

Figure 18 The WAXS melting sequence of PEN

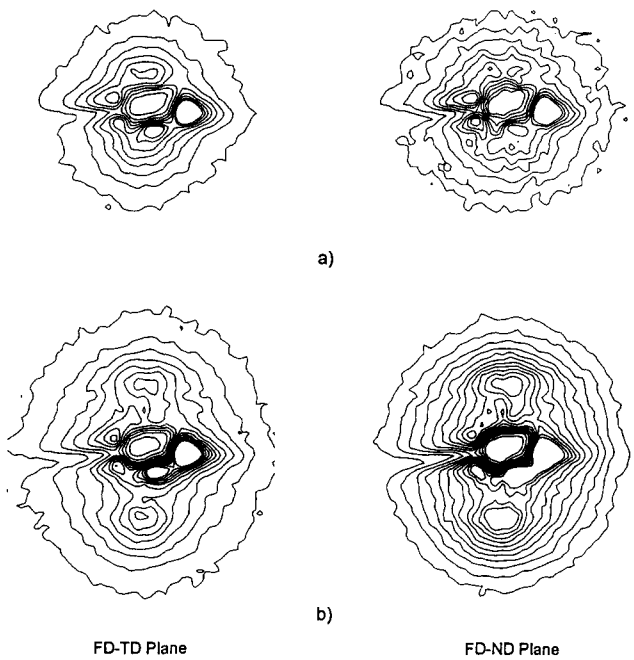

Figure 19 SAXS patterns taken from No. 3 location of PEN samples moulded at (a) 20°C and (b) 180°C using the low injection speed

When the mould temperature was increased to 180°C (*Figure 19b*), two point SAXS pattern characteristic of stacked lamellar type morphology developed in the FD–TD and FD–ND planes. The pattern indicates that lamellar stacks having a long spacing of 238 Å developed during thermal crystallization of PEN at that region.

CONCLUSIONS

Our detailed structural analysis showed that, the amorphous skin-crystalline intermediate-amorphous core type morphology observed in injection moulded PEN can be explained by the competition between the cooling and crystallization rate at a given point in the mould. The stress history (injection speed) and the mould temperature are the main variables that affect this competition. At mould temperatures above the glass transition temperature, the holding time becomes another factor affecting the internal structure due to the enhanced thermally induced crystallization.

In all moulding conditions strong (0 2 0) and ($\bar{1}\,\bar{1}\,1$) planes belonging to the β-crystal form were observed at the intermediate (shear crystallized) regions. This evidence, along with earlier findings[2,8,9] suggest that the crystalline layers are formed under the severe shear stresses acting at the solid melt boundary during the filling stage. This region must be subjected to a temperature window (220–250°C) that satisfies the nucleation range of the β crystals along with a substantial stress field that accelerates their crystallization kinetics. This result is also in agreement with the lowering of the cold crystallization temperature as a consequence of high deformation history, at the same location[10].

It was shown that, in the shear crystallized region, the naphthalene planes are aligned parallel to the ND–TD plane. This observation proves our earlier suggestion[10] that such an alignment will cause the formation of a highly stratified structure. This structure will promote delamination of the shear crystallized layers when subjected to shearing stress as a result of slippage of chains due to lack of inter-molecular links.

In an earlier work[10] we observed that at mould temperatures below the T_g, the mechanical properties of the small dumbbells are insensitive to the moulding conditions. In this paper, we observed that in this temperature range, although the thickness of the crystalline layers changes with increasing mould temperature, the orientation of the naphthalene planes in the crystalline layers remains the same. This preferential orientation is responsible for the delamination of the crystalline layers. These observations imply that the mechanical properties depend on the texture of the crystalline regions, which act as a failure initiator by causing delamination. Since the moulding conditions only affect the thickness of the crystalline layers (and not its presence or absence) the mechanical properties of small dumbbells are naturally insensitive to the moulding conditions.

On the other hand, observations such as the higher melting point crystals, the existence of thread-like structures, low elongation to break, high level of preferential orientation and the lack of discrete SAXS peaks suggest the existence of extended chain crystals in the shear crystallized regions. The results of the hot stage WAXS experiment indicates that these extended chain crystals are a mixture of α and β crystal form.

In this research we saw that the β form could be grown at temperatures below the minimum observed in the quiescent crystallization conditions. There are several possible mechanisms responsible for this.

(1) The first mechanism is the lowering of entropy of crystallization which will reduce the critical nucleus size at a given temperature thus broaden the crystallization range.

(2) The second mechanism is the perfection of the already nucleated crystals that were too small to give distinct diffraction peaks.

(3) The third mechanism is the direct influence of flow on the arrangement of molecules in the crystallized regions. The main difference between the α and β forms is in the spatial arrangement of the naphthalene planes along the chain. In α form, all *trans* conformation is present whereas in β form the naphthalene planes alternately rotate 180°C about the chain axis which in turn make the c-axis shorter as indicated by Buchner

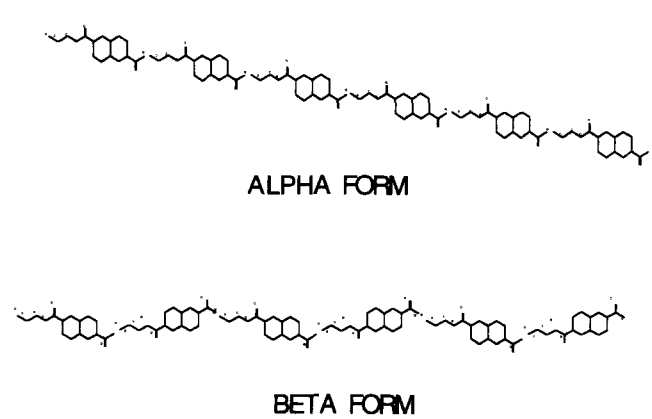

Figure 20 Schematic spatial arrangement of the polymer chains in α and β crystal forms

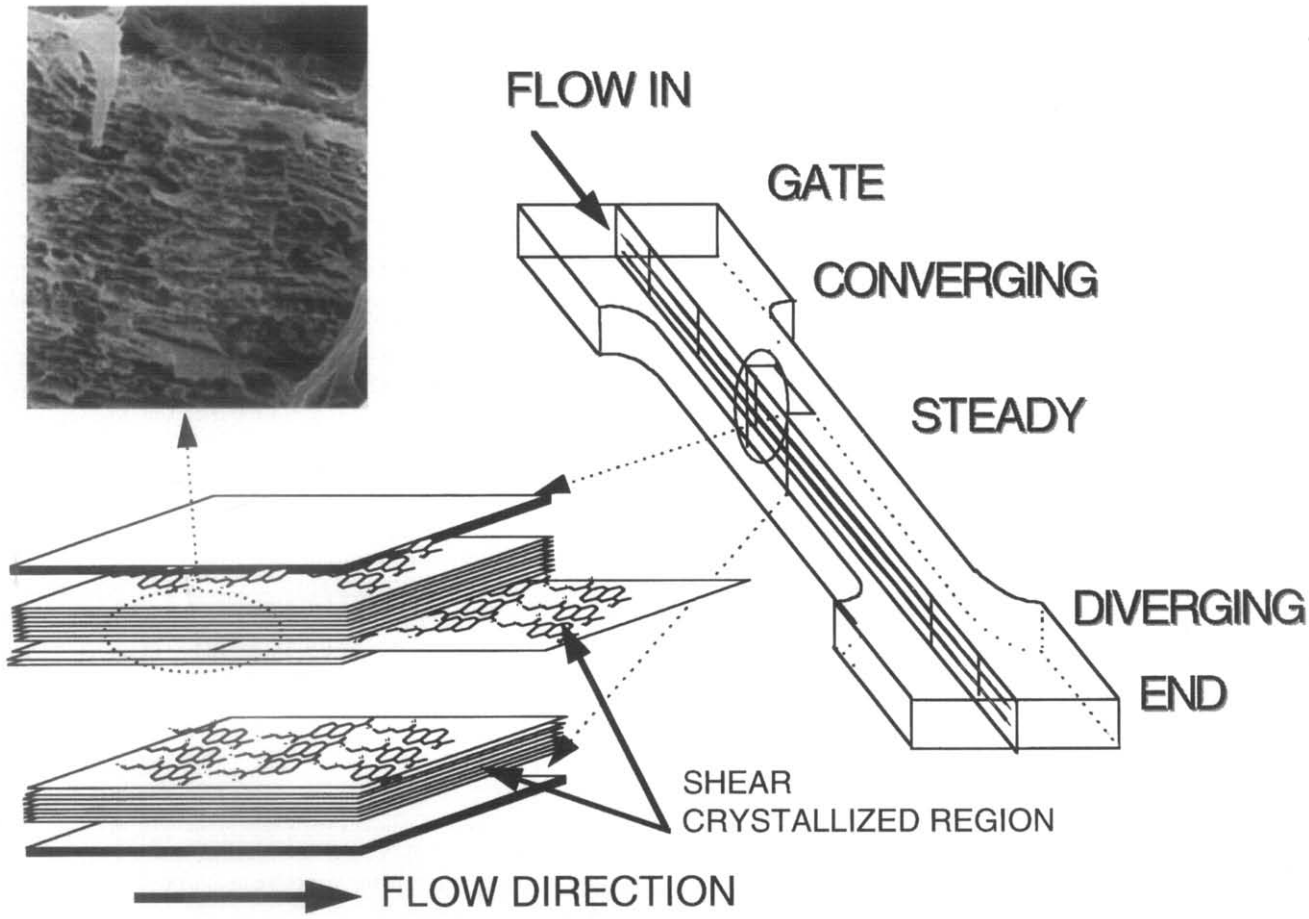

Figure 21 Hierarchical model for the shear crystallized layers in injection moulded PEN

et al.[2] (*Figure 20*). It is suspected that during the filling stage when the crystallization conditions are satisfied, the polymer chains near the crystallizing surface would be subjected to large extensional deformation under the shear field together with rotation (smearing action). In a shear field, these highly planar naphthalene planes would easily align parallel to the shearing plane. This alignment can occur in a given chain with all the naphthalene planes in conformation observed in the α form or in β as the only difference between them is 180° rotation of the naphthalene planes about the chain axis. Under these circumstances the probability of finding chain segments with a sequence of naphthalene planes alternating 180° at each monomer would be smaller and as a result we see that a small fraction of the crystalline region is in β form. The structural hierarchy developed in injection moulded PEN is summarized in *Figure 21* where the results obtained from X-ray and SEM are presented.

ACKNOWLEDGEMENTS

This research was funded in part by M. Cakmak's Presidential Young investigator award from NSF DDM 8858303. The polymer was kindly provided by Dr Bill Boon of Goodyear (now Shell) Polyester division.

REFERENCES

1. Cook, J. G., Hugill, H. P. W. and Lowe, A. R., British Pat. No. 604073, 1948.
2. Buchner, S., Wiswe, D. and Zhachmann, H. G., *Polymer*, 1989, **30**, 480.
3. Mencik, Z., *Chem. Prum.*, 1967, **17**, 78.
4. (a) Teijin Ltd., British Pat. No. 37484/71, 1971. (b) Teijin Ltd., Netherlands Pat. No. 72-16920, 1972.
5. Zachmann, H. G., Wiswe, D., Gehrke, R. and Riekel, C., *Macromol. Chem. Suppl.*, 1985, **12**, 175.
6. Hayashi, S., Ishiharada, M. and Saito, S., *Polym. J.*, 1985, **17**, 953.
7. Cakmak, M., Wang, Y. D. and Simhambhatla, M., *Polym. Eng. Sci.*,1990, **30**, 721.
8. Cakmak, M. and Lee, S. W., *Polymer*, 1995, **36**, 4039.
9. Cakmak, M. and Kim, J. C., *J. Appl. Polymer. Sci.*, submitted.
10. Ulcer, Y. and Cakmak, M., *Polymer*, 1994, **35**, 26.
11. Hoare, L. and Hull, D., *Polym. Eng. Sci.* 1977, **17**, 204.
12. Menges, G. and Wubken, G., *SPE ANTEC Tech. Papers*, 1973, **19**, 519.
13. Katti, S. S. and Schultz, J. M., *Polym. Eng. Sci.*, 1982, **22**, 1001.
14. Fleischmann, E. and Koppelmann, J., *Kunststoffe*, 1987, **77**, 405.
15. Cakmak, M., Wang, Y. D. and Ulcer, Y. (unpublished results).
16. Elsner, G., Riekel, C. and Zachmann, H. G., *Adv. Polym. Sci.*, 1985, **67**, 1.
17. McHugh, A. J., *Polym. Eng. Sci.*, 1982, **22**, 15.
18. White, J. L. and Spruiell, J. E., *Polym. Eng. Sci.*, 1981, **21**, 859.
19. Wilchinsky, Z. W., *J. Appl. Phys.*, 1959, **30**, 792.